ISSN : 0974 - 7486 Volume 13 Issue 1

Materials Science

An Indian Journal

Full Paper

MSAIJ, 13(1), 2015 [022-031]

Studies on the optical properties of ZnO nanostructured thin films synthesized by RF magnetron sputtering

B.Khalfallah*, F.Chaabouni, M.Abaab

Université Tunis El Manar- ENIT - Laboratoire de Photovoltaïque et Matériaux Semiconducteurs, BP 37, Le belvédère 1002, (TUNIS)

E-mail : bilel_khalfallah@yahoo.com

ABSTRACT

Zinc oxide (ZnO) thin films were deposited by RF magnetron sputtering onto glass substrates at room temperature. The thickness effect on the structural, morphological and optical properties of the ZnO filmswasstudied. Films thickness was calculated by interference fringes method and varied from 360 nm to 680 nm. The grain size was in the range of 26 - 29 nmcorresponding to nanostructured films. Stress values at different thickness were investigated. The root mean square roughness of the films increased from 3.3 to 12.2 nm in the thickness range of investigation. The average optical transmittance of the films was about 85 % in the visible region. The optical band gap of the ZnO films decrease from 3.37to 3.09 eV with increasingfilm thickness. The refractive index dispersion and dielectric constants were investigated by Cauchy, Wemple-Didomenico and Spitzer-Fan models. The results demonstrated that the optical properties were highly related to structural ones. The obtained films can be used as transparent electrodes in solar cells.

KEYWORDS

Thin films;
RF magnetron sputtering;
Structural properties;
Optical properties.

INTRODUCTION

Zinc oxide (ZnO) is wide-band gap semiconductor of 3.37 eV at room temperature a high transparency in the visible range. It is very promising II-VI semiconductor for optoelectronic applications in the UV region, especially for solar cells, gas sensors, acoustic devices, transistors and the production of light emitting devices (LEDs)[1-4]. It has a hexagonal wurtzite structure, a natural n-type electrical conductivity and a large exciton binding energy (<"60 meV)[5,6]. Several deposition techniques can be used for the production of ZnO thin films, such as laser ablation[7], RF magnetron sputtering[8], Spray pyrolysis[9] and sol–gel process[10].

In this work, we investigated the effect of the films thickness on the structural, morphological and optical properties of undopedZnO films produced by RF magnetron sputtering and we showed that the optical and dielectric constants are highly related to the structural properties of the films.

EXPERIMENTAL DETAILS

Fabrication of the ZnO thin films

The ZnO thin films were prepared on amorphous glass substrates at room temperature by RF magnetron

sputtering using a ceramic target of pure ZnO (99.999 %) with a thickness of 5 mm anda diameter of 100mm. The Glass substrates were used in this study thanks to their low cost, high transparency, high insulating property and low optical absorption above about 300 nm (for ZnO, absorption edgelocates atabout 360 nm). Before deposition, cleaning of the glass substrates was performed by a soap solution followedby degreasing with acetone in an ultrasonic bath. The substrateswere then rinsed properly with de-ionized water and dried in air. The substrates were rotated (15 rd/mn) and placed parallel to the target surface at a distance of 65 mm. RF magnetron sputtering power was adjusted to 200 W. Inorderto avoidcontaminatingthefilms, the chamber wasevacuatedtoa base pressureofabout 10^{-4}Pa. Argongaswasintroducedintothe chamber throughamassflowcontroller. Themassflowofargon gas wasfixedat2.6 sccm, corresponding to afinalpressureof 1.0Pa. Thetargetwaspre-sputteredfor15mintoremove contaminants. ZnO films with different thicknesses were deposited by varying deposition time. The grown samples are represented using the notations E1, E2, E3 and E4 corresponding to a thicknessof360 nm, 485 nm, 575 nm and680 nm, respectively.

Characterizations of the produced films

Obtained ZnO films were characterized using X-ray diffraction (PANalyticalX'Pert Pro, Philips Co, Ltd) with $Cu\ K_\alpha$ radiation (λ = 0.15406 nm) to identify the crystal structure and orientation of each phase. ASTM table were used for indexing the lines. Film thicknesswas calculated with Swanepoel procedure[11] which is based on the use of the extremes of the interference fringes. Surface morphology was observed using an atomic force microscope (NanoscopeIIIaVeeco type dimension 3100). The optical properties of the films were measured at normal incidence in the wavelength range from 300 to 1800 nm using a double-beam UV-VIS-NIR spectrophotometer (Shimadzu).

RESULTS AND DISCUSSION

Structure characterization

Figure 1 shows the XRD patterns of ZnO films deposited at different thicknesses. All samples exhibit a (0 0 2) peak at 2θ<"34°, indicating that the RF sputteredZnO films have a hexagonal wurtzite structure and show a good c-axis orientation perpendicular to the substrate. The c-axisorientation in ZnO films can be explained by the modelproposed by Drift[12]. According tothis model, nucleation withvarious orientations can be formed at the initial stage of the filmdeposition and each nucleus competes to grow; but only nuclei having the fastest growth rate on the substrate can survive, i.e., c-axis orientation is achieved. The absence of additional peaks in the XRD patterns excludes the possibility of any extra phases and/or large size precipitates in the films. The (0 0 2) ZnO peak intensity increases as the films thickness increases from E1 (360 nm) toE4 (680 nm).

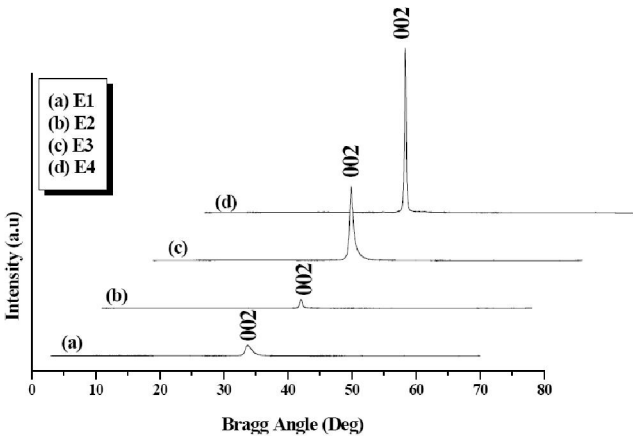

Figure 1 : XRD patterns of ZnO films deposited on glass substrates at different films thickness

To assess the crystal qualityof ZnO films, the grain sizeas a function of film thickness was calculated fromXRD data by Scherrer formula[13]:

$$D = \frac{0.9\lambda}{B\cos\theta} \quad (1)$$

where D is the average grain size, λ is the X-ray wavelength, θ is the diffraction angle of the peak and B is the value of the full width at half maximum (FWHM) of the (002) peak. As film thickness increases, theFWHM decreases from 0.32 to 0.29 and the grain size increases from 26 to 29 nm indicating an enhancement of the crystallinity. Similar behavior was reported by W.L. Dang et *al.*[14] and C. S. Baek et *al.*[15].

The strain ε in ZnO thin films along c-axis perpendicular to thesubstrate was calculated using the equation:

Full Paper

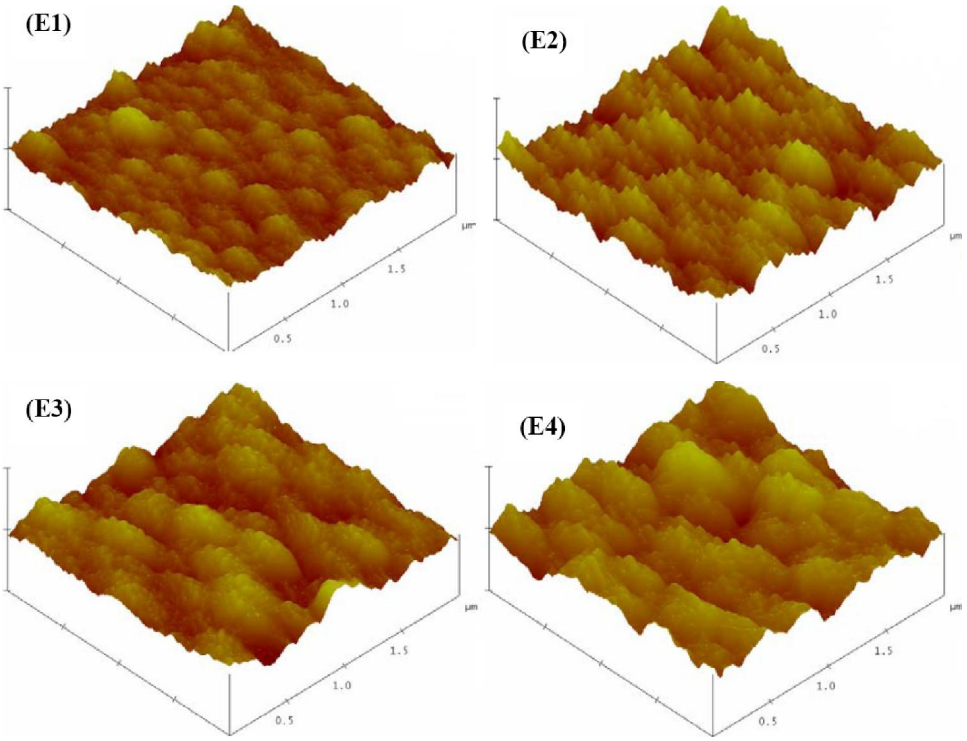

Figure 2 : AFM images of ZnO films at different films thickness (Surface area studied = 2 × 2 µm2)

$$\varepsilon(\%) = \frac{\Delta c}{c_0} \times 100\% \quad (2)$$

where Δc is the difference between the lattice parameter 'c' of the films (calculated from XRD data) and the lattice parameter 'c_0' of unstrained ZnO (5.206Å)[16]. For hexagonal systems, the residual stress σ in the plane of the film can be calculated from the strain (see Eq. (3)) with the biaxial strain model[16]:

$$\sigma = 2C_{13} - \frac{C_{33}(C_{11} + C_{12})}{C_{13}} \times \varepsilon \quad (3)$$

where C_{ij} are the elastic stiffness constants for single ZnOcrystal (C_{11}= 208.8 GPa, C_{33}= 213.8 GPa, C_{12}= 119.7 GPa, C_{13}= 104.2 GPa)[17,18]. The estimated values of stress σ in the grownfilmsare found to decrease from -4.74 to -0.09 GPawith films thickness. The negative stress values indicate that the films are in a state of compressive intrinsic stress[19,20]. The intrinsic stress originates from defects in the films and is thought to be associated with the sputtered particles bombarding the grown film during sputtering process, which will cause lattice distortion of the films to increase the stress[21].

Morphologicalcharacterization

Figure 2 displays the AFM micrographs (2 $\mu m \times 2$ μm) of the ZnO films with various thicknesses. It can be seen that all samplesdemonstrates a uniform and densely packed granular arrangement. Thecrystallite diameter measured using AFM analysis is around 19, 33, 50 and 65 nm for E1, E2, E3 and E4, respectively. The grain size estimated by XRD data and the crystallite size indicating by AFM vary in the same trend indicating that crystallite is composed of small grains surrounded by the grain boundaries. The RMS roughness is gradually increased from 3.30 to 12.23 nm with film thickness. This increase may be related to the larger grain size formation as well as an increase in the grain film porosity[22]. Such an increase of RMS roughness with increasing film thickness was also noticed by R. S. Reddyet *al*.[23]. The increase of RMS roughness of ZnO films leads significant effect on the industrial applications such as gas sensors.

Optical characterization

Figure 3 showsthetransmittance (T) spectra in the wave range of 300 – 1800 nm of theZnO films with different thicknesses. All the spectra reveal very pronounced interference effects in the transparency and NIR regions (400 - 1800 nm) with a sharp fall of trans-

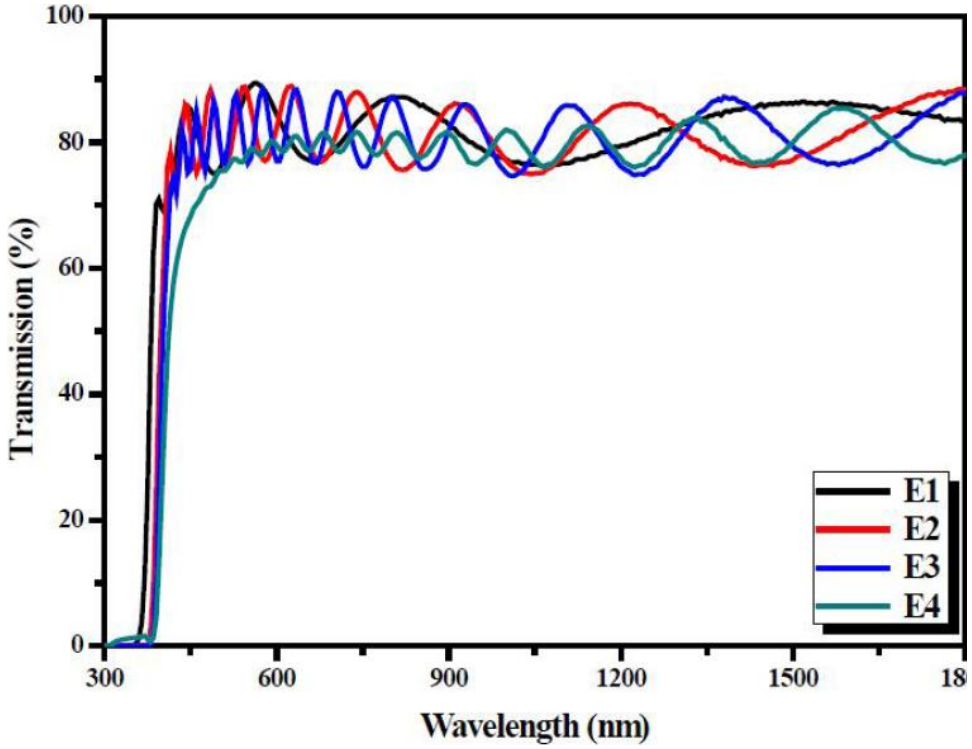

Figure 3 : Optical transmittance spectra of ZnO at differentfilms thickness

mittance at the band edge. All the films are highly transparent with transmittance values in the range of 75 - 90 %. In addition, the reflectance values for all the samples are in the range of 10 - 25 %. This result suggests that these films behave as a transparent material and indicate a good optical quality due to the low absorption losses in the visible and NIR range. Hence, these films can be used as transparent window materials in many optoelectronic devices.

The absorptioncoefficient of the ZnO films isevaluatedfromthe transmittance (*T*) andreflectance (*R*) databyusingthefollowing formula[24]:

$$\alpha = \frac{1}{d} Ln\left[\frac{(1-R)^2}{T}\right](cm^{-1}) \quad (4)$$

where α is the absorption coefficient, *d* is the film thickness and *R* and *T* are the reflection and transmission coefficients, respectively.

Figure 4 shows the dependence of the absorption coefficient on wavelengths for theZnO films with different thicknesses. It can be seen that all the samples have relatively high absorption coefficients (higher than 10^5 cm^{-1} in the UV region). Similar behavior was reported byN. Ekemet *al*.[25]. This result reveals that these films have potential in photovoltaic applications[26]. Furthermore, the strong absorptionregion extends until smaller wavelengths which belong to the UVregion. So, these films are also promising materials for solar protective coatings[27-29].

The optical band gap$E_g$of the films can be determined from the absorptioncoefficient of the films using the relation for parabolicbands[30]:

$$(\alpha h\nu)^2 = A(h\nu - E_g^{\ opt}) \quad (5)$$

where, *hν* is the photon energy, *A* is constant and E_g is the optical band gap. The values of the direct optical band gaps are obtained by plotting $(\alpha h\nu)^2$ as a function of *h* and extrapolating the linear portion of the curve to the energy (*h*) axis.$(h)^2$ versus *h*for the deposited ZnO films are presented in Figure 5. The optical band gap values of the deposited ZnO films are found to decrease from 3.37 to 3.09 eV with film thickness.

The decrease in bandgap values with increasing the films thickness (see Figure 6) can be explainedwith the relaxation of the compressivestress due to longer cycle times as reported by T. Singh et *al*.[31]. Indeed, the compressed lattice is expected to provide a wider bandgap

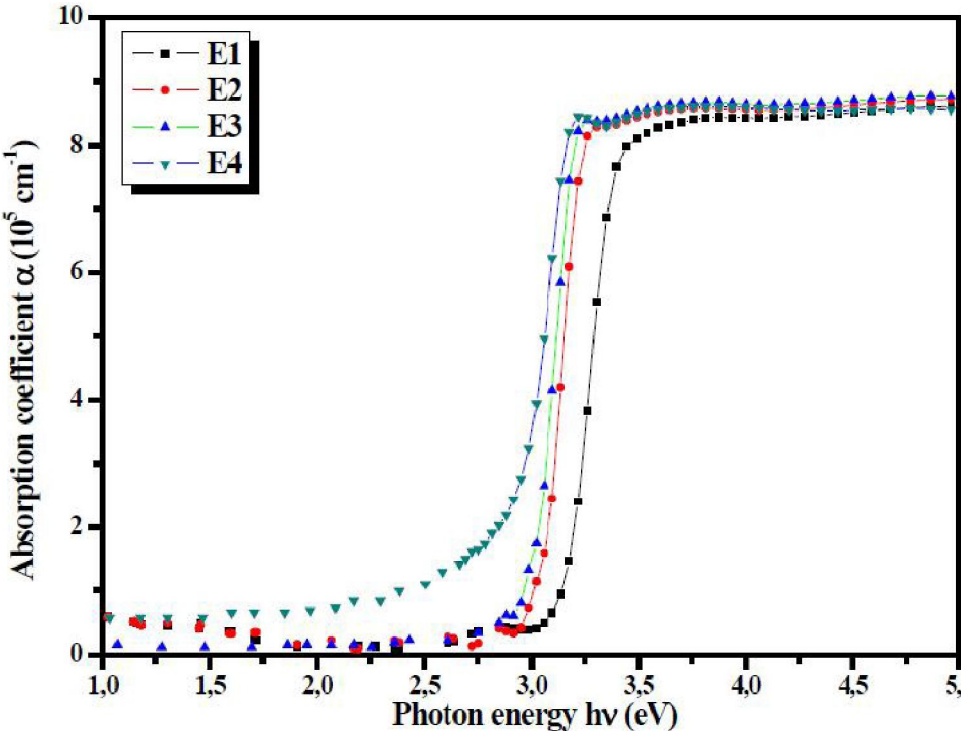

Figure 4 : Absorption coefficient of ZnOat different films thickness

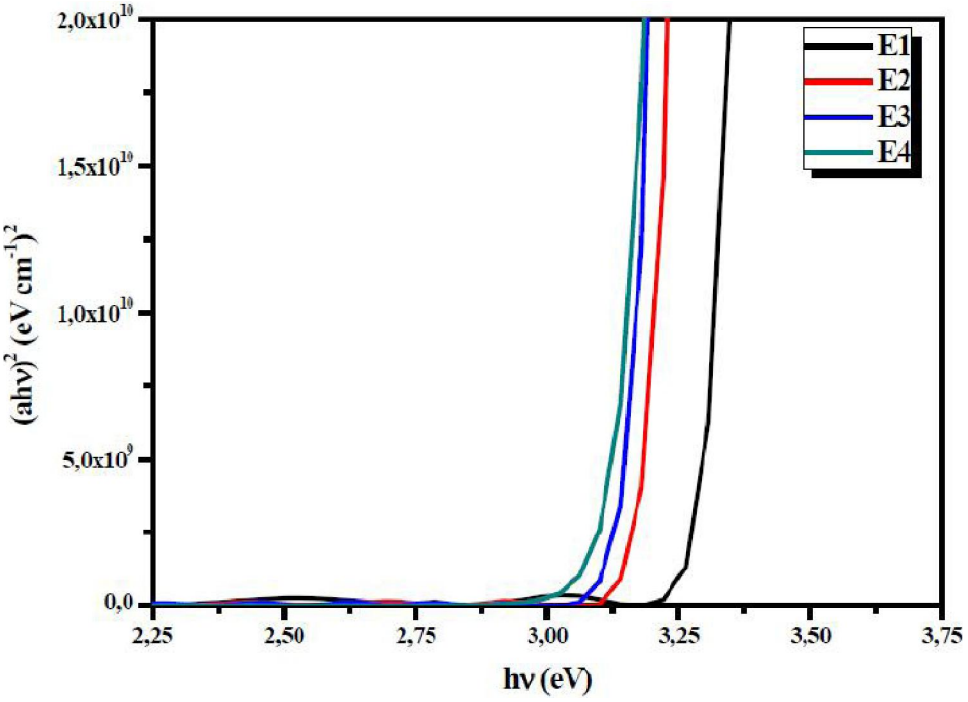

Figure 5 : The Tauc plots of ZnO at different films thickness

because of the increased repulsion between the oxygen *2 p* and the zinc *4s* bands[32].

The refractiveindex *n (λ)* canbedeterminedusingthe transmission envelopesofthinfilmsdeposited on atransparentsubstrate[33]. Using this method, the refractive index is expressedby[34].

$$n = \left[N + (N^2 - S^2)^{1/2} \right]^{1/2} \quad (6)$$

Where

$$N = 2S \frac{T_M - T_m}{T_M T_m} + \frac{S^2 + 1}{2} \quad (7)$$

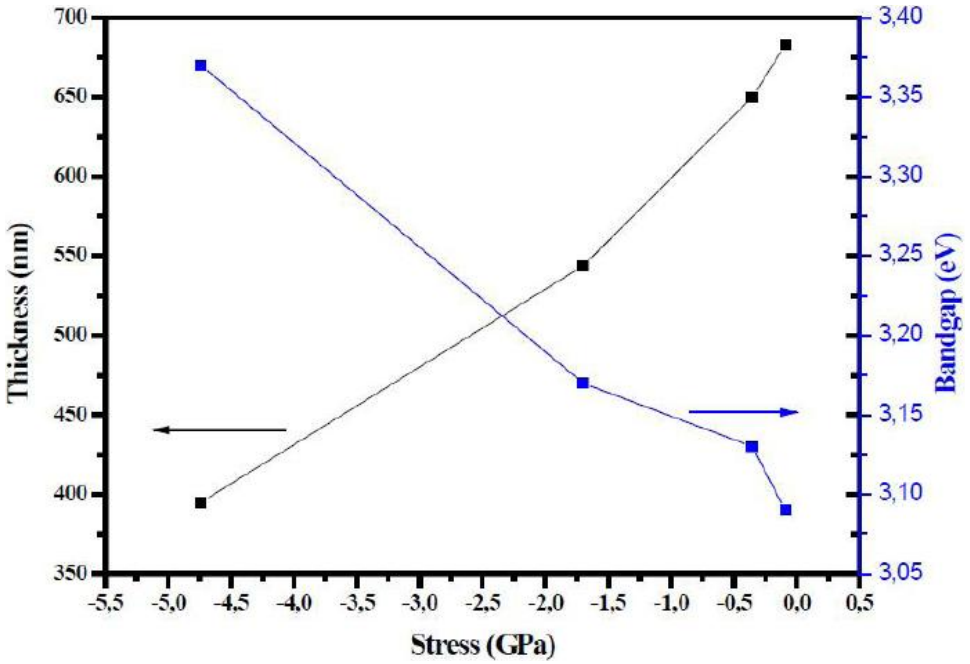

Figure 6 : Stress evolution in ZnO thin films with increasing thickness andbandgap evolution in ZnO thin films with decreasing stress

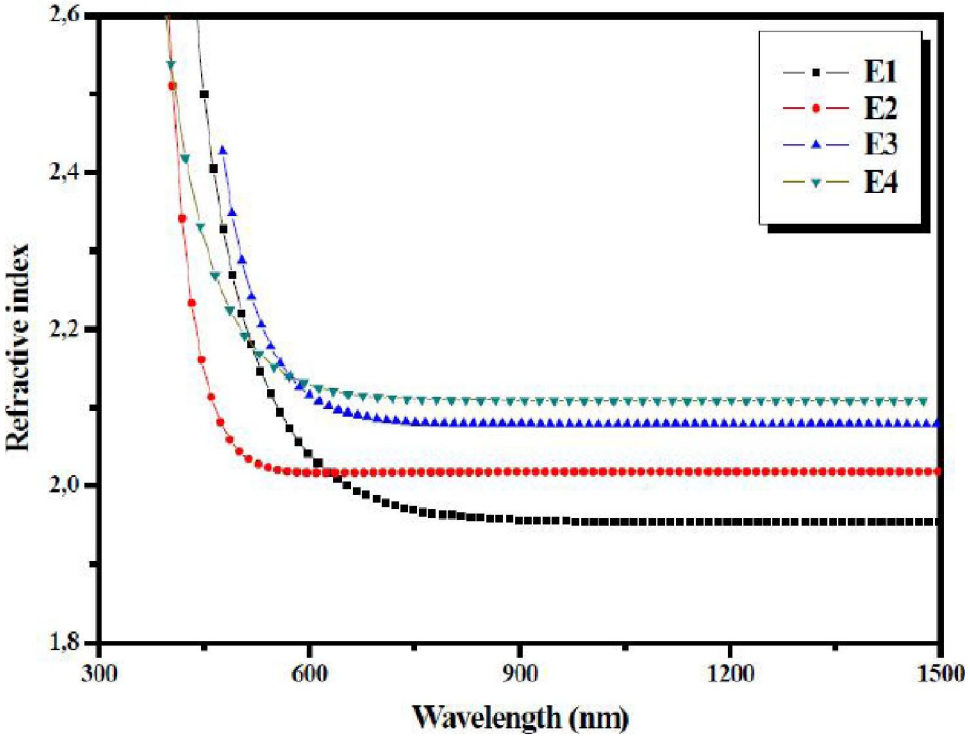

Figure 7 : Refractive index versus wavelength λof ZnO at different films thickness

where *S* is the refractive index of the glass substrate. T_M and T_m are the envelope values at maximum and minimum positions of the transmission spectra, respectively. Figure 7 shows the refractive index evolution as a function of wavelength. It's clear that the refractive index values decrease sharply in the range of 400 – 750 nm thanstabilize in the range of 750 – 1500 nm. The refractive indexes for all samples are found to increase by increasing film thicknesses. This result may be due to the increase in the values of grain size and the improvement in the crystallinity indicating an improvement in films density. With the increase of film thick-

Full Paper

ness, the film becomes denser and denser. $n(\lambda)$ of the deposited ZnO thin films are fitted by the Cauchy model[35]:

$$n(\lambda) = n_0 + \frac{A}{\lambda^2} + \frac{B}{\lambda^4} + \frac{C}{\lambda^6} \quad (8)$$

where $n_{0,c}$, A, B and C are the Cauchy's parameters and is the wavelengthof the light used. The good fit implies that the films have normal dispersion for the entirestudied wavelength range. Theestimatedvaluesof $n_{0,c}$, A, B and C evaluated fromthefittingof $n(\lambda)$ bytheCauchyformulaaretabulated in TABLE1.

The single oscillator Wemple–Didomenico[36,37] was also used to fit the dispersion of refractive index as:

$$n^2(h\nu) = 1 + \frac{E_d E_0}{E_0^2 - (h\nu)^2} \quad (9)$$

where $h\nu$ is the photon energy, E_0 is the single oscillator energy which is a measure of the energy difference between the 'centres of gravity' of the valence and conduction bands and an indicator for the energy gap quantification of the material[38] and E_d is the dispersion energy whichrepresents a measure of the average strength of interband optical transitions. Figure 8 shows plots of $(n^2-1)^{-1}$versus $(h\nu)^2$ and by fitting a straight line, E_0 and $E_d$can be determined directly from slope, $(E_0E_d)^{-1}$ and the interceptE_0/E_d, on the vertical axis. The refractive index $n_{0,w}$ can also be deduced from the dispersion relationship for $(h\nu)$ '! 0, extrapolated fromthe Wemple-Didomenico single oscillator fit.

The estimated values of $n_{0,w}$, E_0 and $E_d$at different films thickness werere grouped in TABLE 1. We note that the values of n_0 found by the Cauchy fitting and the Wemple–DiDomenico modelareingood agreement.

Under the same model, the refractive index can also be analyzed to determine the long wavelength refractive index n_{∞}, average oscillator wavelength $\lambda_0$and oscillator length strength S_0 of each thin film. These values can be obtained by using the following relations[39,40]:

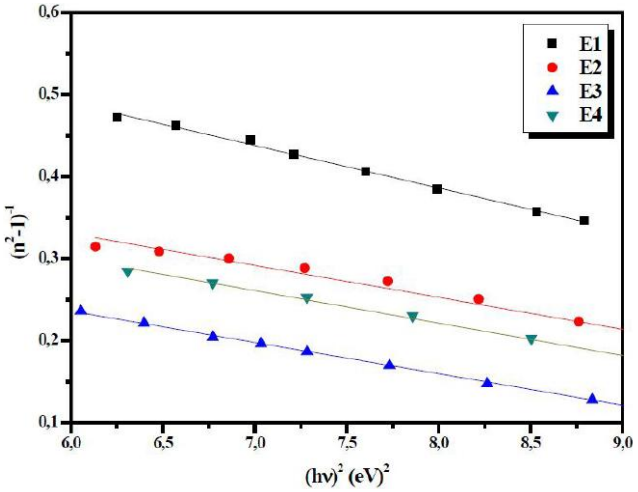

Figure 8 : Plot of*(n2-1)-1* versus *(hv)2* of ZnO at different films thickness forthedeterminationof *n0,n", 5ØßSØßO, S0, E0* and *Ed*

TABLE 1 : Calculated values of Cauchy parameters *n0, A, B*and *C*

	$n_{0,c}$	A (10^5 nm^2)	B (10^{10} nm^4)	C (10^5 nm^6)
1	1.81	0.218	-1.72	7.39
E2	1.94	1.340	-7.76	118.83
E3	2.04	0.941	-6.70	147.25
E4	2.11	1.553	-10.77	203.16

$$\frac{n_\infty^2 - 1}{n^2 - 1} = 1 - \left(\frac{\lambda_0}{\lambda}\right)^2 \quad (10)$$

$$n_\infty^2 = 1 + S_0\lambda_0^2 \quad (11)$$

$$n^2 - 1 = \frac{S_0\lambda_0^2}{1 - \left(\frac{\lambda_0}{\lambda}\right)^2} \quad (12)$$

From Figure 8, we obtain n_{∞} and λ_0 values from the linear part of $1/(n^2-1)$ versus λ^{-2}curve. These values are summarized in TABLE 2.

Using the Spitzer-Fan model[41], certaindielectric constants which are linked to there fractive index $n(\lambda)$, are determined allowing better analyze of

TABLE 2 : Calculated values ofwempleDidomenicoparameters

	E_g (eV)	E_0 (eV)	E_d (eV)	$n_{0,w}$	S_0 (μm^{-2})	λ_0 (μm)	n_∞
E1	3,37	5,73	14,85	1.77	55,28	0,21	1,75
E2	3,17	4,51	10,28	1.90	29,20	0,27	1,80
E3	3,13	3,85	9,95	2.03	26,70	0,28	1,85
E4	3,09	3,95	8, 50	2.15	17,45	0,35	1,90

TABLE 3 : Calculated values of dielectric constants (spitzer-fan model)

	ε_∞	$-4\pi\chi_e$	$N/m^*(10^{49}\ g^{-1}\ cm^{-3})$
E1	7.55	1-16.72	7.16
E2	4.95	0.47-9.87	3.63
E3	4.75	0.43-7.93	2.83
E4	5.00	0.21-4.55	1.52

theopticalpropertiesof thethinfilms.

$$\varepsilon_r = n^2 - k^2 = \varepsilon_\infty - \left[e^2/\pi c^2\right]\left(N/m^*\right)\lambda^2 \quad (14)$$

$$\left[e^2/\pi c^2\right]\left(N/m^*\right)\lambda^2 = -4\pi\chi_e \quad (15)$$

where ε_∞ is the high-frequency dielectric constant in the absence of any contribution from free carrier, k is the

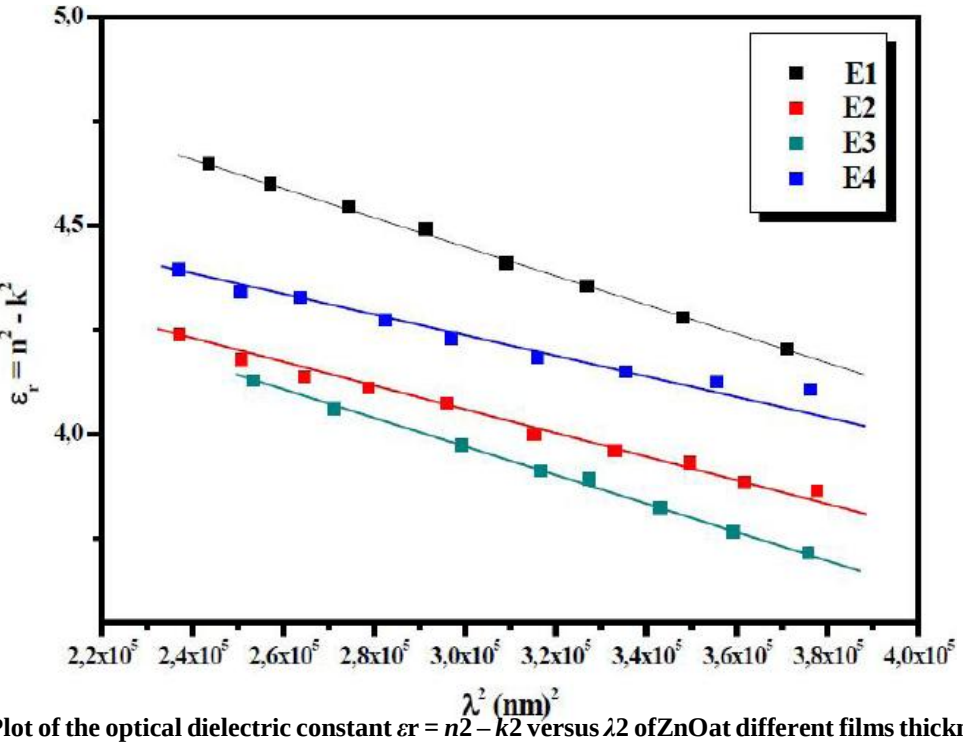

Figure 9 : Plot of the optical dielectric constant $\varepsilon r = n2 - k2$ versus $\lambda 2$ ofZnOat different films thickness

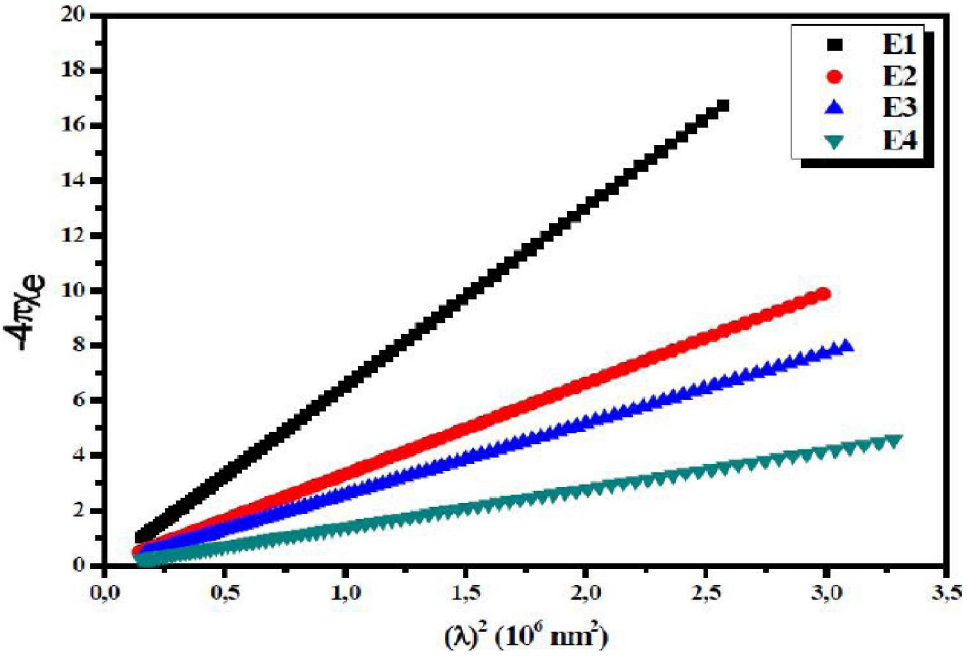

Figure 10 : Plot of ("$4\pi\chi$e) versus $\lambda 2$of ZnO at different films thickness

extinction coefficient, χ_e is the electric free carrier susceptibility, N/m^* is the carrier concentration to the effective mass ratio, e is the electronic charge and c is the velocity of light. The values of $N/m^*$and ε_∞ were estimated by plotting ε_r versus λ^2 (Figure 9) and summarized in TABLE 3.

Figure 10 shows $(''4\pi\chi_e)$ versus λ^2. The figure depicts that χ_e increases in magnitude with the wavelength and becomes sufficiently large to reduce the refractive index and the dielectric constant in the near-infrared region. A good fit to a straight line is seen from which the free carrier susceptibility values at the extremes of the investigated range were estimated.

CONCLUSIONS

In conclusion, we have studied the effect of the thickness on the structural, morphological and optical properties of the ZnO thin films prepared by RF magnetron sputtering. All the samples have a typical hexagonal wurtzite structure with a smooth surface and a growth in a preferred orientation along the direction (002). AFM images showed that the grain size and surface RMS roughness are obviously influenced by the ZnO film thickness. Grain size and RMS roughness increased with increasing thickness. The optical transmittance of ZnO films was over 80 % in the visible region, and red-shift of the optical absorption edge was observed. The optical band gap decreased from 3.37 eV to 3.09 eV with increasing thickness from 360to 680 nm. We usedthe models of Cauchy, Wemple–Didomenico and Spitzer–Fan for the analysis of the dispersion of the refractive index and the determination of the optical and dielectric constants. These studies show thatZnO has excellent optical properties for solar cell applications as antireflection coating.

REFERENCES

[1] R.Ebrahimifard, M.R.Golobostanfard, H.Abdizadeh; Applied Surface Science, **290**, 252–259 **(2014)**.

[2] R.Vettumperumal, S.Kalyanaraman, R.Thangavel; Journal of Molecular Structure, **1059**, 61–67 **(2014)**.

[3] Y.E.Jeong, S.Park; Current Applied Physics, **14**, 30-33 **(2014)**.

[4] R.Sridhar, C.Manoharan, S.Ramalingam, S.Dhanapandian, M.Bououdina; SpectrochimicaActa Part A: Molecular and Biomolecular Spectroscopy, **120**, 297–303 **(2014)**.

[5] L.Ma, X.Ai, X.Huang, S.Ma; SuperlatticesMicrostruct., **50**, 703–712 **(2011)**.

[6] C.F.Wang, B.Hub, H.H.Yia; Optik, **123**, 1040–1043 **(2012)**.

[7] E.Fazio, A.M.Mezzasalma, G.Mondio, T.Serafino, F.Barreca, F.Caridi; Appl.Surf.Sci., **257**, 2298–2302 **(2011)**.

[8] F.Gao, X.Y. Liu, L.Y.Zheng, M.X.Li, Y.M.Bai, J.Xie; J.Cryst.Growth, **371**, 126–129 **(2013)**.

[9] S.Benramache, B.Benhaoua; SuperlatticesMicrostruct., **52**, 1062–1070 **(2012)**.

[10] P.Jongnavakit, P.Amornpitoksuk, S.Suwanboon, T.Ratana; Thin Solid Films, **520**, 5561–5567 **(2012)**.

[11] R.Swanepoel; J.Phys., **16**, 1214 **(1983)**.

[12] V.A.Drift; Philips Res.Rep., **22**, 267 **(1967)**.

[13] B.E.Warren; X-ray Diffraction, Dover, New York **(1990)**.

[14] W.L.Dang, Y.Q.Fu, J.K.Luo, A.J.Flewitt, W.I.Milne; Superlattices and Microstructures, **42**, 89–93 **(2007)**.

[15] C.S.Baek, D.H.Kim, H.H.Kim, K.J.Lim; Journal of Ceramic Processing Research., **132**, 403-406 **(2012)**.

[16] H.C.Ong, A.X.E.Zhu, G.T.Du; Appl.Phys.Lett., **80**, 941–943 **(2002)**.

[17] B.D.Cullity, S.R.Stock; Elements of X-ray Diffractions, 3, Prentice Hall, Engle-wood Cliffs, NJ, **(2001)**.

[18] R.Kumar, N.Khare, V.Kumar, G.L.Bhalla; Appl.Surf.Sci., **254**, 6509–6513 **(2012)**.

[19] R.Kumar, N.Khare, V.Kumar, G.L.Bhalla; Applied Surface Science, **254**, 6509–6513 **(2008)**.

[20] T.Singh, T.Lehnen, T.Leuning, D.Sahu, S.Mathur; Applied Surface Science, **289**, 27– 32 **(2014)**.

[21] B.L.Zhu, S.J.Zhu, J.Wang, J.Wua, D.W.Zeng, C.S.Xie; Physica E, **43**, 1738–1745 **(2011)**.

[22] N.Kakani, S.H.Jee, S.H.Kim, J.Y.Oh, Y.S.Yoon; Thin Solid Films, **519**, 494 **(2010)**.

[23] R.S.Reddy, A.Sreedhar, A.Sivasankar Reddy, S.Uthanna; Adv.Mat.Lett., **3**, 239-245 **(2012)**.

[24] D.E.Milovzorov, A.M.Ali, T.Inokuma, Y.Kurata, T.Suzuki, S.Hasegawa; Thin Solid Films, **382**, 47 **(2001)**.

[25] N.Ekem, S.Korkmaz, S.Pata, M.Z.Balbag, E.N.Cetin, M.Ozmumcu; international journal of hydrogen energy, **34**, 5218–5222 **(2009)**.

[26] C.Bauer, G.Boschloo, E.Mukhtar, A.Hagfeldt; Chem.Phys.Lett., **387**, 176–181 **(2004)**.
[27] S.S.Shariffudin, M.Salina, S.H.Herman; Transactions On Electrical And Electronic Materials, **13**, 102-105 **(2012)**.
[28] L.Miao, S.Tanemura, M.Tanemura, S.P.Lau, B.K.Tay; J.Mater.Sci.Mater.Electron., **18**, 343–346 **(2007)**.
[29] G.X.Liang, P.Fan, X.M.Cai, D.P.Zhang, Z.H.Zheng; Journal Of Electronic Materials, **40 (2011)**.
[30] J.I.Pankove; Optical Processes in Semiconductors, Dover, New York **(1971)**.
[31] T.Singh, T.Lehnen, T.Leuning, D.Sahu, S.Mathur; Applied Surface Science, **289**, 27– 32 **(2014)**.
[32] R.Ghosh, D.Basak, S.Fujihara; J.Appl.Phys., **96**, 2689–2692 **(2004)**.
[33] E.Marquez, J.B.Ramirez-Malo, P.Villares, R.Jimenez-Garay, R.Swanepoel; Thin Solid Films, **254**, 83 **(1995)**.
[34] R.Swanepoel; Journal of Physics E: Scientific Instruments, **17**, 896 **(1984)**.
[35] H.G.Tompkins, W.A.McGahan; Spectroscopic Ellipsometry and Reflectometry, John Wiley & Sons Inc. **(1999)**.
[36] S.H.Wemple, M.Di Domenico; Phys.Rev.B, **143**, 1338 **(1971)**.
[37] S.H.Wemple; Phys.Rev.B, **7**, 3767 **(1973)**.
[38] F.Skuban, S.R.Lukic, D.M.Petrovic, I.O.Gúth; Journal of Non-Crystalline Solids, **355**, 2059–2062 **(2009)**.
[39] A.K.Wolaton, T.S.Moss; Proc.R.Soc.A, **81**, 5091 **(1963)**.
[40] P.A.Lee, G.Said, R.Davis, T.H.Lim; J.Phys.Chem.Solids, **30**, 2719–2729 **(1969)**.
[41] W.G.Spitzer, H.Y.Fan; Phys.Rev., **106**, 882 **(1957)**.